

Extremely large-scale Array Systems: Near-Filed Codebook Design and Performance Analysis

Feng Zheng

Abstract—Extremely large-scale Array (ELAA) promises to deliver ultra-high data rates with more antenna elements. Meanwhile, the increase of antenna elements leads to a wider realm of near-field, which challenges the traditional design of codebooks. In this paper, we propose novel codebook design schemes which provide better quantized correlation with limited overhead. First, we analyze the correlation between codewords and channel vectors uniform linear array (ULA) and uniform planar array (UPA). The correlation formula for the ULA channel can be expressed as an elliptic function, and the correlation formula for the UPA channel can be represented as an ellipsoid formula. Based on the analysis, we design a uniform sampling codebook to maximize the minimum quantized correlation and a dislocation ULA codebook to reduce the number of quantized bits further. Besides, we give a better sampling interval for the codebook of the UPA channel. Numerical results demonstrate the appealing advantages of the proposed codebook over existing methods in quantization bit number and quantization accuracy.

Index Terms—ELAA, codebook, correlation fitting formula, near-field, quantization bits

I. INTRODUCTION

Massive multiple-input multiple-output (MIMO) technology is a vital component of fifth-generation (5G) mobile communication networks. MIMO involves the utilization of multiple antennas to concentrate signal power within a limited area, contributing to enhanced energy efficiency and spectral efficiency [1], [2]. However, with the explosive increase of demand on data rates in the forthcoming sixth-generation (6G) mobile communication networks, current massive MIMO cannot meet the requirement because congregating enough signal power with limited antennas is difficult. To address this issue, ELAA technology, comprising hundreds or thousands of antennas, is considered as a crucial enabling technology for next generation communication [3]. ELAA enables efficient multiplexing of multiple user equipment (UE) on the same time-frequency resource, thereby improving spectral efficiency and data rates. Additionally, the deployment of ELAA's high beamforming gain facilitates enhanced spatial resolution and compensates for significant path loss experienced in the terahertz frequency bands [4].

Although more antenna elements in ELAA bring benefits in spectral efficiency and data rates, side effects on wireless channel characteristics brought by the increasing antenna numbers also demand attention. The electromagnetic field is generally divided into far-field and near-field, and their boundaries can be determined by the Rayleigh distance $2D^2/\lambda$, where D represents the array size and λ represents the wavelength [6]. Due to the deployment of ELAA and high-frequency carriers, the Rayleigh distance is extended to tens

to hundreds of meters, so UE is more likely to locate in the near-field [7]. For example, for a 128×128 UPA operating at 100 GHz, the near-field region extends to 490 meters.

The high beamforming gain of the ELAA system heavily relies on the accurate channel state information (CSI) at the transmitter [9]. Especially in the radiating near-field, the non-negligible distance factor poses a significant challenge to the precise alignment of the beams [10]. In the time division duplex (TDD) system, the uplink and downlink have reciprocity, and downlink CSI can be obtained through uplink channel estimation. However, for the frequency division duplex (FDD) system, the uplink and downlink work on different frequencies, which makes the channel reciprocity very weak, so it is difficult to deduce the downlink CSI from the uplink CSI [11]. That is, CSI can only be obtained through dedicated feedback provided by UE over signaling channels of limited capacity [12].

Currently, there are two typical categories of CSI acquisition methods, the explicit CSI acquisition and the implicit CSI acquisition. Explicit feedback schemes directly report an element-wise quantized channel vector. They allow for more flexible transmission or reception methods, which can achieve a higher scheduling gain. However, explicit feedback requires a higher overhead than implicit feedback, so implicit feedback can enable more accurate link adaptation [13]. A mainstream technique in implicit feedback is the codebook-based approach, which feeds back an index of a quantized CSI in a pre-designed codebook to the transmitter. For codebook-based feedback, the quantization accuracy of CSI depends on the codebook structure and the allowed number of feedback bits [14]. The existence of massive antennas and non-negligible distance dimension in ELAA leads to an unexpected increase in pilot overhead. Therefore, it is crucial to design a codebook to achieve accurate quantization of CSI with limited feedback considering the near-field channel characteristics of ELAA.

A. Related Works

Extensive researches have focused on the design of far-field codebooks. The far-field electromagnetic wave can be considered a plane wave, so the phase changes linearly with the antenna index. The 5G new radio (NR) standard adopted a discrete Fourier transform (DFT) codebook for the ULA system, and the two-dimensional DFT (2D-DFT) codebook was introduced for the UPA system [15]. Moreover, to enable more accurate CSI acquisition, the NR standard supported codebook oversampling and the linear combination of multiple codewords for feedback [16]. IEEE 802.16 m standard adopted

an adaptive codebook structure, such as the skewed codebook, and a differential codebook structure, such as a Polar-Cap codebook [17]. Besides, in the case of low pilot overhead, the hierarchical codebook [18], angle-of-departure (AoD) adaptive subspace codebook [19], and compressed sensing (CS) [20] methods could also be utilized to quantify CSI accurately. Among them, the codebook feedback schemes based on CS utilize the sparsity of the channel in the angle domain to achieve the goal of low feedback overhead.

Only some studies have focused on codebook design for large near-field ELAA systems. [21] designed a codebook for the near-field UPA, which uniformly samples in real space. However, significant quantization errors exist in quantizing the channel in real space. Besides, [22] derived a one-dimensional (1D) near-field beamforming codebook design, which locates the codeword quantization point based on the Lloyd-Max algorithm. The scheme in [22] improved the near-field beamforming gain, but this scheme still needed to give a theoretical analysis of the codebook quantization performance.

Meanwhile, near-field CSI quantization and feedback have been studied in some research. [23] designed a new polarization-domain codebook for near-field ULA and a CS feedback method based on the sparsity of the polar domain. Considering both angle and distance information, a new polarization-domain codebook for near-field ULA and a CS feedback method based on the sparsity of the channel in the polar domain was designed. This method used the on-grid polar-domain simultaneous orthogonal matching pursuit (P-SOMP) algorithm and the off grid polar-domain simultaneous iterative gridless weighted (P-SIGW) algorithm CS algorithm to feedback near-field channel information. In [24], a hierarchical codebook was designed by projecting the near-field channel into the angle and slope domains, considering the incomplete coverage and overlap of spatial chirp beams, further designing a hierarchical codebook via manifold optimization and alternative minimization.

To our knowledge, no studies have analyzed the correlation between near-field channels. The correlation is sensitive to angle and distance in the near-field polarization domain. Correlation performs distinctive change patterns in near-field and far-field. Unfair sampling methods will make codewords redundant and reduce quantization accuracy. In addition, there are few studies on the codebook and channel feedback scheme of the UPA channel. The UPA channel has one more angle parameter than the ULA channel, significantly increasing the codeword overhead. Therefore, a codebook suitable for near-field channels needs to be carefully designed.

B. Contributions

To fill in this gap, in this paper, we analyze the quantization performance in theory and propose codebook design schemes for the ULA channel and the UPA channel in the ELAA system. Our main contributions are summarized as follows

- We provide a theoretical analysis of the relationship between codeword quantization performance and quantization region in ULA and UPA channels. Specifically,

we derive a polynomial form of the correlation formula between the codeword and the channel. The correlation formula for the ULA channel can be expressed as an elliptic function, and the correlation formula for each codeword remains constant, which indicates its stability. Besides, the correlation formula for the UPA channel can be represented as an ellipsoid formula, and the correlation formulas for different codewords vary, indicating non-stationarity. The polynomial expression of the correlation formula facilitates the design of sampling between codewords.

- We propose two codebook design methods for ULA and UPA, respectively. Based on the correlation formula of the ULA codebook, a uniform sampling codebook scheme with maximized minimum correlation is given. Furthermore, we propose an improved dislocation sampling scheme that reduces the number of quantized codewords. Considering the non-stationary correlation in the UPA channel, we propose a sampling scheme that achieves an upper bound on the codeword quantization performance. Analytical results show that oversampling in the angle domain can achieve higher quantization performance. In near-field channels, the number of quantized bits of CSI is nonlinearly proportional to the number of BS antennas.

C. Organization and Notation

The remainder of the paper is organized as follows. Section II presents the system model. Section III analyzes the characteristic of correlation, and describes the polynomial fitting formula in both ULA and UPA model. In Section IV, the near-field optimal uniformly codebook and uniformly dislocation codebook of ULA channel are proposed. Section V presents the optimal codebook design method of UPA channel and evaluates the proposed codebook. Simulation results are provided in Section VI, and conclusions are drawn in Section VII.

Notations: Vectors are denoted by lowercase bold letters, while matrices are denoted by uppercase bold letters; \otimes denotes the Kronecker product; $(\cdot)^H$ and $(\cdot)^T$ denotes the conjugate-transpose and diagonal operations, respectively; $\Upsilon_{(m,n)}$ denotes the (m,n) -th entry of the matrix Υ ; Υ_n denotes the n -th column of the matrix Υ ; v_n denotes the n -th element of the vector v .

II. SYSTEM MODEL

In this section, we describe the system model of the near-field ELAA communication system. First, we introduce the spherical wave model of ELAA system. Next, we present a CSI quantization feedback model, and formulate the design of the codebook as an optimization problem.

A. ULA Near-field Channel Model

Consider a downlink narrow-band ELAA system, where the BS is equipped with a ULA to serve a single antenna UE. As shown in Fig. 1, the N -antenna array is placed along

the y -axis. The antenna spacing is $d = \lambda/2$, where λ is the electromagnetic wavelength. The coordinate of the n -th antenna is given by $\mathbf{t}_n = (0, y_n)$, where $y_n = (n - \frac{N+1}{2})d$ with $n = 1, 2, \dots, N$. Meanwhile, the UE is located at $\mathbf{u} = (r \cos \theta, r \sin \theta)$, where r and θ represent the distance and angle between UE and array center, respectively.

The line-of-sight (LoS) channel is considered because this paper only focuses on the quantization feedback problem of the near-field codebook. According to the spherical wave model [23], the distance determines the signal phase, and the near-field channel vector \mathbf{h} can be expressed as

$$\mathbf{h} = \sqrt{N}g\mathbf{b}(r, \theta), \quad (1)$$

where $g = \sqrt{\eta}e^{-jk r}/r$ is the complex-valued channel gain with η and $k = 2\pi/\lambda$ denoting the reference channel gain at a distance of $1m$ and wave number, respectively. $\mathbf{b}(r, \theta)$ denotes the beam focusing vector, which is given by

$$\mathbf{b}(r, \theta) = \frac{1}{\sqrt{N}} \left[e^{-jk(r_1-r)}, e^{-jk(r_2-r)}, \dots, e^{-jk(r_N-r)} \right]^T, \quad (2)$$

where $r_n = \|\mathbf{t}_n - \mathbf{u}\|$ represents the distance between the n -th antenna at the BS and the UE. Furthermore, according to the second order Taylor series expansion $\sqrt{1+x} = 1+x/2 - x^2/8 + \mathcal{O}(x^3)$, r_n can be approximated as

$$\begin{aligned} r_n &= \sqrt{(r \sin \theta - y_n)^2 + (r \cos \theta)^2} \\ &\approx r - \sin \theta y_n + \frac{\cos^2 \theta}{2r} y_n^2. \end{aligned} \quad (3)$$

Therefore, the n -th element of near-field beam focusing vector \mathbf{b} can be simplified as

$$b_n = \frac{1}{\sqrt{N}} e^{-jk \left(-\sin \theta y_n + \frac{\cos^2 \theta}{2r} y_n^2 \right)}. \quad (4)$$

Remark 1: When the r is sufficiently large, the $\cos^2 \theta / 2r$ term can be omitted, and $\mathbf{b}(r, \theta)$ is simplified as

$$\mathbf{a}(\theta) = \frac{1}{\sqrt{N}} \left[1, e^{j\pi \sin \theta}, \dots, e^{j\pi(N-1) \sin \theta} \right]^T, \quad (5)$$

which is equivalent to the conventional far-field beam steering vector for the ULA. And the DFT codebook is adopted to quantify the far-field channel vector. Therefore, to be more precise, the concept of “near-field” in this paper does not exclude far-field as well.

B. UPA Near-field Channel Model

As shown in Fig. 2, the BS employs a UPA, which is located on the xOy plane and the center of the array is located at the coordinate origin. $N \times N$ uniformly spaced antenna elements are placed in both horizontal and vertical directions, with a spacing of $d = \lambda/2$. The Cartesian coordinate of the (m, n) -th antenna element of the UPA can be expressed as $\mathbf{t}_{(m,n)} = (x_m, y_n, 0)$ with $x_m = (m - \frac{N+1}{2})d$, $y_n = (n - \frac{N+1}{2})d$, $m = 1, \dots, N$, $n = 1, \dots, N$. Meanwhile, we assume the coordination of UE is $\mathbf{u} = (r \sin \theta \cos \phi, r \sin \theta \sin \phi, r \cos \theta)$, where r , θ and ϕ represent the distance, elevation angle and azimuth angle of UE relative to the UPA center, respectively. Therefore, the

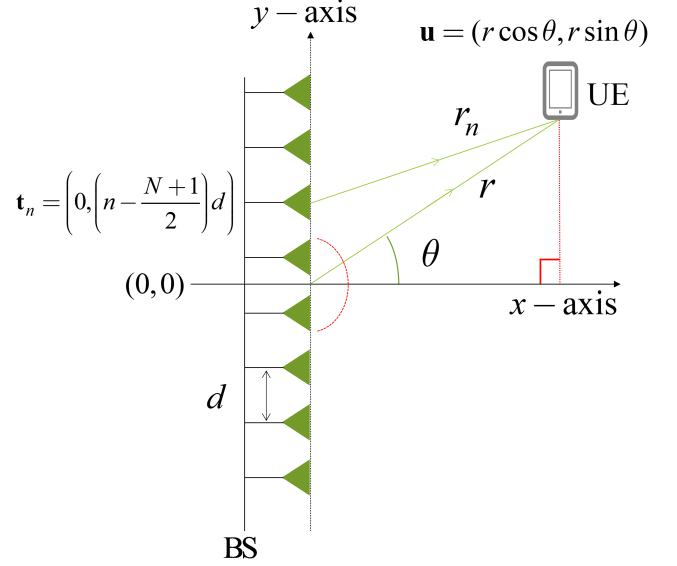


Fig. 1: Near-field channel model for ULA communication system.

beam focusing vector for UPA can be obtained based on the spherical wave propagation model as

$$\mathbf{b}(r, \theta, \phi) = \frac{1}{N} \left[e^{-jk(r_{(1,1)}-r)}, \dots, e^{-jk(r_{(N,N)}-r)} \right]^T, \quad (6)$$

where $r_{(m,n)} = \|\mathbf{t}_{(m,n)} - \mathbf{u}\|$ represents the distance between the (m, n) -th antenna at the BS and the UE, which can be approximated as

$$\begin{aligned} r_{(m,n)} &\approx r - \sin \theta \cos \phi x_m - \sin \theta \sin \phi y_n \\ &\quad + \frac{1 - \sin^2 \theta \cos^2 \phi}{2r} x_m^2 + \frac{1 - \sin^2 \theta \sin^2 \phi}{2r} y_n^2 \\ &\quad - \frac{\sin^2 \theta \cos \phi \sin \phi}{r} x_m y_n. \end{aligned} \quad (7)$$

As a result, the (m, n) -th element of the LoS channel can be represented as

$$b_{(m,n)} = \frac{1}{N} e^{-jk(r_{(m,n)}-r)}. \quad (8)$$

Remark 2: When the r is sufficiently large, the last 3 terms in (7) can be omitted, and $\mathbf{b}(r, \theta, \phi)$ is simplified as

$$\begin{aligned} \mathbf{a}(\theta, \phi) &= \frac{1}{N} \left[1, \dots, e^{j\pi(m \sin \theta \cos \phi + n \sin \theta \sin \phi)}, \dots, \right. \\ &\quad \left. e^{j\pi((N-1) \sin \theta \cos \phi + (N-1) \sin \theta \sin \phi)} \right]^T, \end{aligned} \quad (9)$$

which is equivalent to the conventional far-field beam steering vector for the UPA, and the 2D-DFT codebook is adopted for the CSI feedback. Since the phase of (9) can be decoupled into two parts in terms of x and y , the 2D-DFT codebook can be expressed in the form of the Kronecker product of the DFT vectors, that is

$$\mathbf{a} = \mathbf{a}_x \otimes \mathbf{a}_y, \quad (10)$$

where $\mathbf{a}_x = \frac{1}{\sqrt{N}} [1, e^{j\pi \sin \theta \cos \phi}, \dots, e^{j\pi(N-1) \sin \theta \cos \phi}]^T$ and $\mathbf{a}_y = \frac{1}{\sqrt{N}} [1, e^{j\pi \sin \theta \sin \phi}, \dots, e^{j\pi(N-1) \sin \theta \sin \phi}]^T$. However, the cross-term $\sin^2 \theta \cos \phi \sin \phi x_m y_n / r$ in (7) prevents

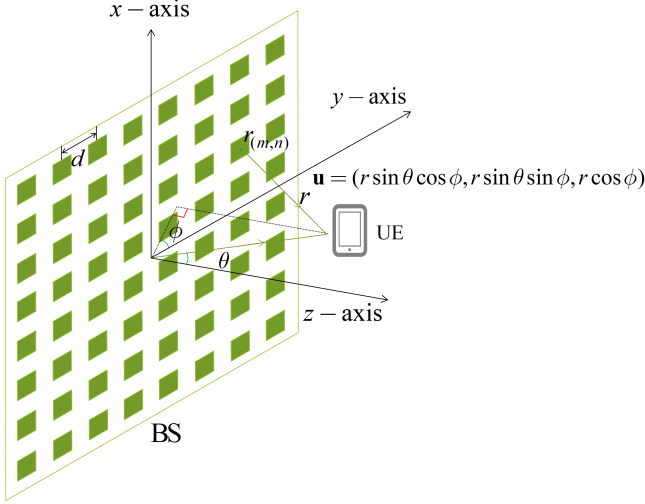


Fig. 2: Near-field channel model for UPA communication system.

it from being decoupled as $\mathbf{a}(\theta, \phi)$. Therefore, the near-field codebook for the UPA cannot be directly constructed based on the ULA codebook, which will be explained in detail later.

C. CSI Quantization Feedback Model

For FDD communication systems, the BS can obtain the CSI through the UE's feedback. Specifically, the pilot signal $\mathbf{X} = \text{diag}(x_1, \dots, x_{\tilde{N}})$ is transmitted at first, where x_n denotes the pilot symbol for the n -th antenna, and \tilde{N} represents the size of either ULA or UPA. At the UE side, the received signal is given by

$$\mathbf{y} = \mathbf{X}\mathbf{h} + \mathbf{n}, \quad (11)$$

where \mathbf{n} is the additive Gaussian white noise (AWGN) with variance σ^2 . Based on this, the estimation of channel vector, denoted as $\hat{\mathbf{h}}$, can be obtained by methods such as least squares (LS) [25]. Since this paper mainly focuses on the codebook design for the near-field communication, the perfect CSI estimation is assumed, i.e., $\hat{\mathbf{h}} = \mathbf{h}$.

To inform the BS of CSI with limited feedback, the channel vector is quantized based on a predefined codebook $\mathbf{W} = [\mathbf{W}_1, \dots, \mathbf{W}_S]$, which contains S codewords and satisfies $\|\mathbf{W}_s\| = 1$. The UE selects the ideal codeword from the codebook and feeds back its index $s^* = \arg \max_s |\mathbf{h}^H \mathbf{W}_s|^2$ to the BS. Finally, the BS can determine the transmission scheme based on the CSI feedback from the UE. For example, the codeword \mathbf{W}_{s^*} can be utilized as the beamforming weight.

In the above quantization feedback model, the codebook design affects the channel quantization accuracy, which in turn affects the performance of the communication system. Obviously, all the channel vectors in the region of interest have different correlations with the codewords. This paper considers the max-min correlation criterion, and assuming

$\mathcal{W} = \{\mathbf{W}_1, \dots, \mathbf{W}_S\}$, the near-field codebook design problem can be formulated as

$$\begin{aligned} \max_{\mathbf{W}} \min_{\mathbf{h} \in \mathcal{H}} \max_s |\mathbf{h}^H \mathbf{W}_s| \\ \text{s.t. } |\mathcal{W}| = S. \end{aligned} \quad (12)$$

or

$$\begin{aligned} \min_{\mathcal{W}} |\mathcal{W}| \\ \text{s.t. } \min_{\mathbf{h} \in \mathcal{H}} \max_s |\mathbf{h}^H \mathbf{W}_s| > c. \end{aligned} \quad (13)$$

\mathcal{H} represents the set of LoS channel vectors within the region of interest, and c represents the correlation between codewords and channel vectors.

In the above quantization feedback model, the codebook design affects the channel quantization accuracy, which in turn affects the performance of the communication system. Obviously, all the channel vectors in the region of interest have different correlations with the codewords. This paper considers the max-min correlation criterion, and assuming $\mathcal{W} = \{\mathbf{W}_1, \dots, \mathbf{W}_S\}$, the near-field codebook design problem can be formulated as

III. CODEWORD QUANTIZATION PERFORMANCE ANALYSIS

This section first investigates the correlation between the codewords and the near-field channel vectors. The transform domain perspective for analyzing correlation function is proposed, demonstrating many desired mathematical properties. Second, this section gives the fitting formula of the quantization performance of the codeword to the channel vector, which inspires the codebook design.

A. Correlation Function for ULA systems

When codewords are selected from the beam focusing vectors, i.e., $\mathbf{W}_s = \mathbf{b}(r_s, \theta_s)$, they can be viewed as a LoS channel vectors at specific locations. For the ULA systems, the correlation between the codeword $\mathbf{b}(r_s, \theta_s)$ and the beam focusing vector $\mathbf{b}(r_q, \theta_q)$ can be calculated as

$$\begin{aligned} \tau(r_s, \theta_s; r_q, \theta_q) &= |\mathbf{b}^H(r_s, \theta_s) \mathbf{b}(r_q, \theta_q)| \\ &= \frac{1}{N} \left| \sum_{n=1}^N \exp \left(-j \frac{2\pi}{\lambda} \left((\sin \theta_q - \sin \theta_s) y_n \right. \right. \right. \\ &\quad \left. \left. + \left(\frac{\cos^2 \theta_s}{2r_s} - \frac{\cos^2 \theta_q}{2r_q} \right) y_n^2 \right) \right|. \end{aligned} \quad (14)$$

Let $\alpha_i = \lambda \cos^2 \theta_i / 4r_i$, $\beta_i = \sin \theta_i$ with $i = s, q$, (14) can be simplified as

$$\begin{aligned} f(\alpha_s, \beta_s; \alpha_q, \beta_q) \\ &= \frac{1}{N} \left| \sum_{n=1}^N \exp \left(-j\pi \left((\alpha_s - \alpha_q) n^2 + ((\beta_q - \beta_s) \right. \right. \right. \\ &\quad \left. \left. - (\alpha_s - \alpha_q)(N+1)n \right) \right) \right|. \end{aligned} \quad (15)$$

Further, let δ_α and δ_β respectively represent as the location difference between $\mathbf{b}(r_q, \theta_q)$ and \mathbf{W}_s , which can be expressed as

$$\begin{aligned}\delta_\alpha &= \alpha_q - \alpha_s, \\ \delta_\beta &= \beta_q - \beta_s.\end{aligned}\quad (16)$$

Then, (15) can be simplified as

$$f(\delta_\alpha, \delta_\beta) = \frac{1}{N} \left| \sum_{n=1}^N \exp \left(-j\pi \left(-\delta_\alpha n^2 + (\delta_\beta + \delta_\alpha(N+1))n \right) \right) \right|. \quad (17)$$

Without loss of generality, the correlation between the codeword and the channel vector always satisfies $f(\delta_\alpha, \delta_\beta) \leq 1$. $f(\delta_\alpha, \delta_\beta) = 1$ if and only if $\delta_\alpha = 0$ and $\delta_\beta = 0$. Consequently, there is always a certain quantization error when a codeword quantizes a channel other than itself.

To consider the influence of wavelength and number of antennas on the correlation function, we set $\tilde{\delta}_\alpha = \delta_\alpha N^2$ and $\tilde{\delta}_\beta = \delta_\beta N$. For the antenna with a sufficiently large of N , the above formula can be approximated to

$$\tilde{f}(\tilde{\delta}_\alpha, \tilde{\delta}_\beta) \approx \left| \int_{-1/2}^{1/2} \exp \left(-j\pi (\tilde{\delta}_\beta t - \tilde{\delta}_\alpha t^2) \right) dt \right|. \quad (18)$$

(18) converts the coordinate from $(\delta_\alpha, \delta_\beta)$ to $(\tilde{\delta}_\alpha, \tilde{\delta}_\beta)$. The change in the number of antennas N does not affect the expression of $f(\tilde{\delta}_\alpha, \tilde{\delta}_\beta)$. Thus, (18) shows that the channel correlation function is suitable for different antenna numbers N and wavelengths λ , in other words, (17) can be used to describe the correlation between codeword and channel in both the far-field and near-field. Under different correlations c , the difference between the locations satisfying the condition is distributed in contour lines on the α - β domain, as shown in Fig. 3. The correlation between the codeword and the channel vector is only related to the difference in position. Under different correlations c , the difference between the locations satisfying the condition is distributed in contour lines.

Similar to the far-field DFT beam pattern in the angle domain, the correlation function (14) can also be understood as the normalized beam pattern of the near-field beam in the α - β domain. In Fig. 3, the yellow ellipse in the center reflects the beamwidth under a specific correlation requirement. The beamwidth on the α domain is inversely proportional to N^2 , and the beamwidth on the β domain is inversely proportional to N .

Unfortunately, the exponential term in (17) is relatively complicated. Most existing literature deals with the exponential term based on the Fresnel integral [23]. However, it is still difficult to directly obtain the numerical characteristic for the correlation function approximated by the Fresnel integral. Inspired by this, we further explore the correlation properties of codewords. We can deduce the following properties based on the correlation (17).

Property 1 (Stationarity): The correlation between the codeword and channel vector is only related to δ_α and δ_β . For different codeword \mathbf{W}_s and $\mathbf{W}_{s'}$, the correlation's distribution

of codeword with the channel within its quantization region is always the same. The stationarity in the ULA channel can be formulated as

$$\begin{aligned}f(\alpha_s, \beta_s; \alpha_s + \delta_\alpha, \beta_s + \delta_\beta) \\ = f(\alpha_{s'}, \beta_{s'}; \alpha_{s'} + \delta_\alpha, \beta_{s'} + \delta_\beta).\end{aligned}\quad (19)$$

Property 2 (Symmetry): Similar to the symmetry of the DFT beam in the angle domain, the correlation distribution of the near-field channel also satisfies symmetry. In the quantization area of the codeword, the distribution of the correlation between the codeword and the channel is symmetrical about the codeword in the α and β domain, which can be expressed as

$$f(\delta_\alpha, \delta_\beta) = f(\delta_\alpha, -\delta_\beta) = f(-\delta_\alpha, \delta_\beta) = f(-\delta_\alpha, -\delta_\beta). \quad (20)$$

Proof 1: (17) can be rewritten as

$$f(\delta_\alpha, \delta_\beta) = \frac{1}{N} \left| \sum_{n=1}^N \exp \left(-j\frac{2\pi}{\lambda} \left(\delta_\beta y_n - \frac{2}{\lambda} \delta_\alpha y_n^2 \right) \right) \right|. \quad (21)$$

Set $\delta'_\beta = -\delta_\beta$, the above formula can be calculated as

$$f(\delta_\alpha, \delta'_\beta) = \frac{1}{N} \left| \sum_{n=1}^N \exp \left(-j\frac{2\pi}{\lambda} \left(-\delta_\beta y_n - \frac{2}{\lambda} \delta_\alpha y_n^2 \right) \right) \right|. \quad (22)$$

y_n is symmetric about $y_n = 0$ in $[-(N-1)d/2, (N-1)d/2]$, hence there always exists $y_{N-n+1} = -y_n$. Thus, formula (22) can be written as

$$\begin{aligned}f(\delta_\alpha, -\delta_\beta) \\ = \frac{1}{N} \left| \sum_{n=1}^N \exp \left(-j\frac{2\pi}{\lambda} \left(\delta_\beta y_{N-n+1} - \frac{2}{\lambda} \delta_\alpha y_{N-n+1}^2 \right) \right) \right|,\end{aligned}\quad (23)$$

which indicates that $f(\delta_\alpha, \delta_\beta) = f(\delta_\alpha, -\delta_\beta)$. It is evident that $f(\delta_\alpha, \delta_\beta) = f(-\delta_\alpha, -\delta_\beta)$ by central symmetry. Therefore, we can easily deduce that $f(\delta_\alpha, \delta_\beta) = f(-\delta_\alpha, \delta_\beta)$. ■

According to these two properties, we can obtain the correlation characteristics of any codewords by analyzing the correlation of a specific codeword. These features provide convenience for designing the sampling interval between codewords to ensure an ideal design. Next, we will use a polynomial function to approximate the correlation function in Proposition 1.

Proposition 1: When $\delta_\alpha \neq 0$ and $\delta_\beta \neq 0$, the polynomial fitting formula of $f(\delta_\alpha, \delta_\beta)$ can be expressed as

$$f(\delta_\alpha, \delta_\beta) \approx p_\alpha \delta_\alpha^2 N^4 + p_\beta \delta_\beta^2 N^2 + 1, \quad (24)$$

where

$$\begin{aligned}p_\alpha &= -0.025983670363830, \\ p_\beta &= -0.391749735984250.\end{aligned}\quad (25)$$

To sum up, if the correlation between the codeword \mathbf{W}_s and the beam focusing vector $\mathbf{b}(\alpha_q, \beta_q)$ is $f(\delta_\alpha, \delta_\beta) = c \in (0, 1)$, the distribution satisfied by δ_α and δ_β can be equivalent to

$$p_\alpha \delta_\alpha^2 N^4 + p_\beta \delta_\beta^2 N^2 = c - 1. \quad (26)$$

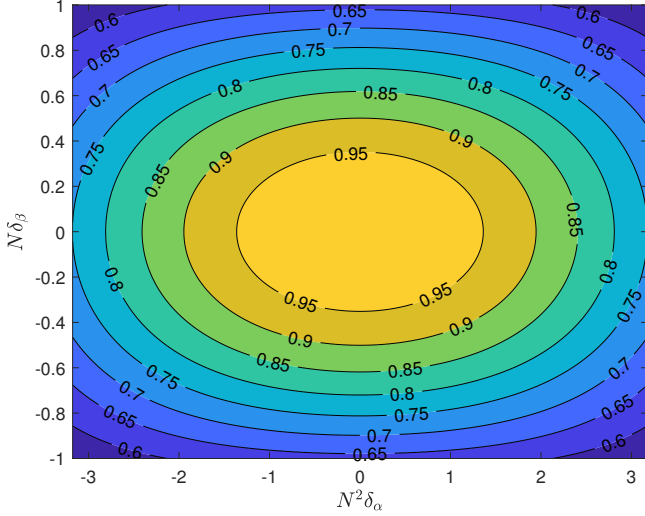


Fig. 3: Contour distribution between codeword quantization correlation and position difference with $f = 3\text{GHz}$ and $N = 512$.

This formula can be further simplified into the form of the following formula

$$\frac{p_\alpha \delta_\alpha^2 N^4}{c-1} + \frac{p_\beta \delta_\beta^2 N^2}{c-1} = 1. \quad (27)$$

Evidently, the correlation fitting formula in Proposition 1 is an elliptic function. The ellipse formula always centers around (α_s, β_s) . Moreover, the ellipse is the quantization boundary of \mathbf{W}_s when the quantization accuracy of the codeword satisfies c . The correlation c affects the major and minor axes of the ellipse formula. The larger c is, the shorter the axial length of the ellipsoid is, and the smaller the codeword quantization area is. Conversely, the minor c is, the axis length of the ellipse is smaller, and the lower the quantization accuracy of the codeword is. Further, the axis length of the ellipse is also decided by N . The axis length of the ellipse in the α and β domains are inversely proportional to N^2 and N , respectively. The formula in Proposition 1 is more concise and easier to calculate than the approximated Fresnel integral function and provides strong theoretical support for the codebook design scheme in this paper. In the next section, we will design ULA codebooks based on the above Proposition 1.

For $\mathbf{W}_0 = \mathbf{b}(0, 0)$, $f(\delta_\alpha, \delta_\beta)$ can be written as $f(\alpha_q, \beta_q)$. At this time, (27) is the quantization boundary of \mathbf{W}_0 and gives the channel vector $\mathbf{b}(\alpha_q, \beta_q)$ which meet the conditions of $|\mathbf{W}_0^H \mathbf{b}(\alpha_q, \beta_q)| = c$. For the codeword \mathbf{W}_0 with the minimum correlation as c , the possible channel vectors $\mathbf{b}(\alpha_q, \beta_q)$ always distribute in the ellipse interior, which can be formulated as

$$\Omega = \left\{ \mathbf{b}(\alpha_q, \beta_q) \left| \frac{p_\alpha N^4 \alpha_q^2}{c-1} + \frac{p_\beta N^2 \beta_q^2}{c-1} \leq 1 \right. \right\}. \quad (28)$$

Considering the stationarity characteristics, the correlation between any codeword and its quantization channel vector can be described using the contour lines shown in Fig. 3.

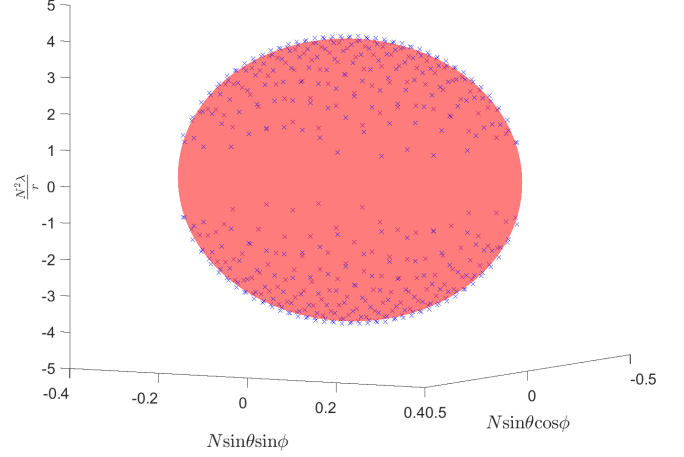


Fig. 4: Correlation distribution plot at \mathbf{W}_0 .

B. Correlation Function for UPA systems

In the UPA system, the correlation between codeword $\mathbf{W}_s = \mathbf{b}(r_s, \theta_s, \phi_s)$ and beam focusing vector $\mathbf{b}(r_q, \theta_q, \phi_q)$ can be calculated as

$$\tau(r_s, \theta_s, \phi_s; r_q, \theta_q, \phi_q) = |\mathbf{b}^H(r_s, \theta_s, \phi_s) \mathbf{b}(r_q, \theta_q, \phi_q)|. \quad (29)$$

We replace the difference of location between the codeword and channel vector as follows

$$\begin{aligned} \delta_{\psi_s} &= \sin \theta_s \cos \phi_s - \sin \theta_q \cos \phi_q, \\ \delta_{\varphi_s} &= \sin \theta_s \sin \phi_s - \sin \theta_q \sin \phi_q, \\ \delta_{\rho_s} &= \frac{1}{r_s} - \frac{1}{r_q}. \end{aligned} \quad (30)$$

Then, (29) can be written as

$$\begin{aligned} &f(\delta_{\psi_s}, \delta_{\varphi_s}, \delta_{\rho_s}) \\ &= \frac{1}{N^2} \left| \sum_{n=1}^N \sum_{m=1}^N \exp \left(-j \frac{2\pi}{\lambda} \left(x_m \delta_{\psi_s} + y_n \delta_{\varphi_s} \right. \right. \right. \\ &\quad \left. \left. - \frac{(1 - (\delta_{\psi_s})^2) \delta_{\rho_s}}{2} x_m^2 - \frac{(1 - (\delta_{\varphi_s})^2) \delta_{\rho_s}}{2} y_n^2 \right. \right. \\ &\quad \left. \left. + (1 - \delta_{\psi_s} \delta_{\varphi_s}) x_m y_n \right) \right|. \end{aligned} \quad (31)$$

The cross-term $x_m y_n$ contained in the UPA channel vector makes it impossible to use the Kronecker product to decouple the channel vector. If the cross-term $x_m y_n$ is ignored, it will cause a significant performance error due to missing more CSI. Before giving the method to solve the above problems, the characteristics of UPA channel correlation shown in the property 3 and property 4 are firstly given.

Property 3 (non-stationarity): The non-stationarity manifests in that the quantized areas of different codewords are not fixed under the minimum correlation c . Therefore, codebooks in UPA channels do not exhibit stationarity. For two codewords

\mathbf{W}_s and $\mathbf{W}_{s'}$, the non-stationarity manifests can be formulated as

$$\begin{aligned} f(\psi_s, \varphi_s, \rho_s; \psi_s + \delta\psi_s, \varphi_s + \delta\varphi_s, \rho_s + \delta\rho_s) \\ \neq f(\psi_{s'}, \varphi_{s'}, \rho_{s'}; \psi_{s'} + \delta\psi_s, \varphi_{s'} + \delta\varphi_s, \rho_{s'} + \delta\rho_s). \end{aligned} \quad (32)$$

Property 4 (symmetry): Symmetry similar to ULA, it is easy to prove that

$$\begin{aligned} f(\delta\psi_s, \delta\varphi_s, \delta\rho_s) &= f(-\delta\psi_s, \delta\varphi_s, \delta\rho_s) = f(\delta\psi_s, -\delta\varphi_s, \delta\rho_s) \\ &= f(-\delta\psi_s, -\delta\varphi_s, \delta\rho_s). \end{aligned} \quad (33)$$

Unlike the ULA model, the non-stationarity of the UPA model brings challenges to the codeword design of UPA. In proposition 2, we give the UPA channel correlation fitting formula different from the ULA fitting formula.

Proposition 2: When $\delta\psi_s \neq 0$, $\delta\varphi_s \neq 0$ and $\delta\rho_s \neq 0$, the correlation between channels in the UPA channel model can be better fitted by a polynomial function, and the fitting formula can be written as

$$\begin{aligned} f(\delta\psi_s, \delta\varphi_s, \delta\rho_s) \\ = p_\psi \delta\psi_s^2 N^2 + p_\varphi \delta\varphi_s^2 N^2 + p_\rho \delta\rho_s^2 N^4 + 1. \end{aligned} \quad (34)$$

If $f(\delta\psi_s, \delta\varphi_s, \delta\rho_s) = c$ and $c \in (0, 1)$, the above formula can be converted into the following ellipsoid formula

$$\frac{p_\psi N^2 \delta\psi_s^2}{c-1} + \frac{p_\varphi N^2 \delta\varphi_s^2}{c-1} + \frac{p_\rho N^4 \delta\rho_s^2}{c-1} = 1. \quad (35)$$

The ellipsoid fitting formula in Proposition 2 gives the quantization boundary of the codeword \mathbf{W}_s with the minimized correlation is c . At a fixed position, the smaller c is, the smaller the axial length of the ellipsoid will be. It should be noted that due to the non-stationary characteristics of the UPA channel, the values of the coefficients p_ψ , p_φ and p_ρ in (34) are related to the specific position of the codeword sampling point and the minimum correlation c . Thus, the ellipsoid fitting formula has different axial lengths for different codewords. The correlation fitting formula in Proposition 2 provides strong support for the codebook design of near-field UPA.

Below we give an example to verify the accuracy of Proposition 2. We plot the actual beam focusing vector whose correlation with the codeword $\mathbf{W}_0 = \mathbf{b}(0, 0, 0)$ satisfies $f(0, 0, 0; \psi_q, \varphi_q, \rho_q) = 0.95$. We calculate the appropriate fitting coefficients from the simulation and plot the corresponding ellipsoid images in Fig. 4, which shows that the actual beam focusing vector satisfying the condition points to the fitted ellipsoid curve. For the codeword \mathbf{W}_0 with the minimum correlation as c , the quantized channel vectors always is distributed in the ellipsoid interior, which can be formulated as

$$\Omega = \left\{ \mathbf{b}(\psi_q, \varphi_q, \rho_q) \left| \frac{p_\psi N^2 \psi_q^2}{c-1} + \frac{p_\varphi N^2 \varphi_q^2}{c-1} + \frac{p_\rho N^4 \rho_q^2}{c-1} \leq 1 \right. \right\}. \quad (36)$$

This example shows that the fitting formula of the UPA channel can more accurately describe the channel correlation of UPA.

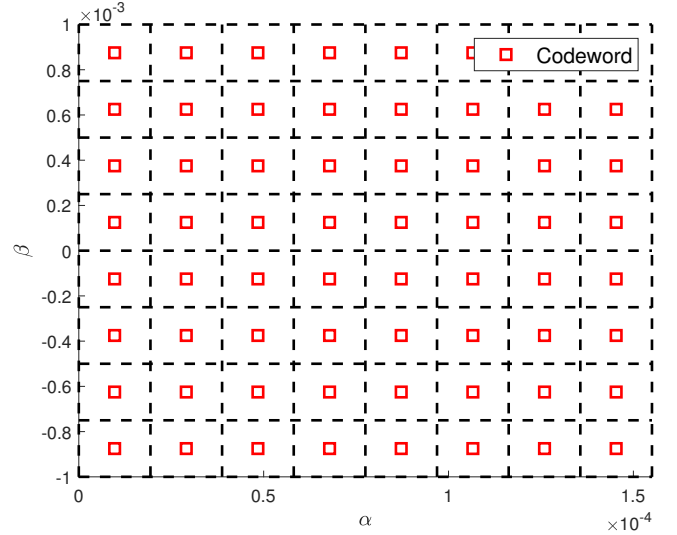


Fig. 5: Uniform codewords on the α - β domain.

IV. NEAR-FIELD ULA CODEBOOK DESIGN

We have analyzed the effect of the angle and distance between the UE and the antenna on the quantization accuracy of codewords. In this section, we describe two quantized codebook design schemes of the ULA channel to ensure the optimal beam gain according to the ULA channel correlation distribution characteristics presented in Section III-A. First, an optimal uniform codebook scheme is proposed, which achieves the maximum quantization range under a minimum correlation. In addition, we redesign a codebook scheme with constant offset in the transform domains to reduce the quantization overhead of the codebook further.

A. Uniform Quantization Codebook Design Scheme

The most commonly used way to obtain the quantified location of the codewords is to perform uniform sampling on the α - β domain, as shown in Fig. 5. α domain and β domain are sampled with S_α and S_β points, respectively. The number of sampling points is $S = S_\alpha S_\beta$, and the index of the codeword is s . Let Ξ^L denote the collection of codeword sampling points, which can be represented as

$$\begin{aligned} \Xi^L = \left\{ (\alpha_s, \beta_s) \left| \alpha_s = \alpha_{min} + \frac{\Delta\alpha}{2}, \alpha_{min} + \frac{3\Delta\alpha}{2}, \dots, \alpha_{max}; \right. \right. \\ \left. \left. \beta_s = \beta_{min} + \frac{\Delta\beta}{2}, \beta_{min} + \frac{3\Delta\beta}{2}, \dots, \beta_{max} \right\}. \end{aligned} \quad (37)$$

where $[\alpha_{min}, \alpha_{max}]$ and $[\beta_{min}, \beta_{max}]$ are the total quantization intervals of the codeword on the α domain and the β domain respectively. $\Delta\alpha$ and $\Delta\beta$ represent the sampling steps on the α and β domain respectively.

Next, we present an in-depth analysis of the distribution performance of the codewords in Fig. 6 to explore the optimal codebook design scheme. The blue triangle is the intersection of the quantization intervals of adjacent codewords, located on the same correlation contour line for each codeword. The correlation contour line where the blue triangle is situated is the outermost correlation contour line of the four

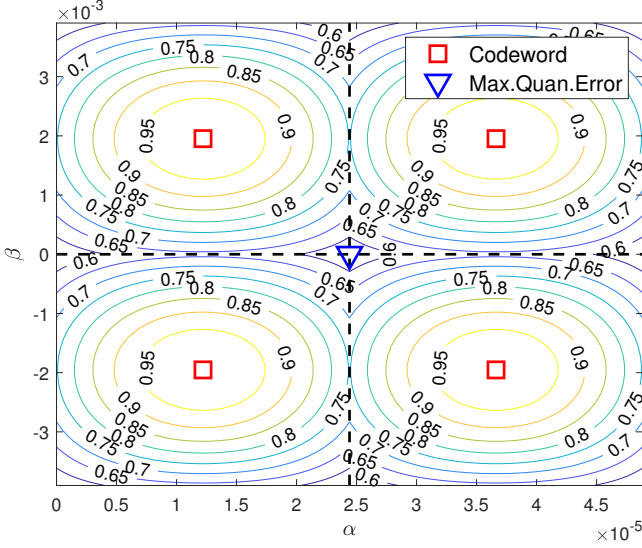


Fig. 6: Correlation distribution of four adjacent uniform sampling points.

codewords, representing the quantization boundary of the codeword. Extending the distribution characteristics to the entire α - β domain, as shown in Fig. 6, the spacing between adjacent codewords is always symmetrical about the minimum correlation point of the codeword.

Furthermore, we reveal the relationship between codeword quantization regions and codeword quantization accuracy for individual codewords in the α - β domain with the constant minimum quantization error. As shown in Fig. 7, the quantization area of the codeword is rectangular with uniform sampling points. The vertices of the rectangular region are located on the minimum correlation contour line. Multiple layouts of rectangular vertices on the minimum correlation contour line constitute quantization schemes with different areas. In order to improve the accuracy of codeword quantization CSI, the minimum correlation of each codeword quantization is always expected to be as large as possible. Therefore, the target can be mapped as the area of the rectangle enclosed by the four quantization boundaries is the largest on a specific ellipse contour line.

According to Cauchy's inequality, for any point on the ellipse (27), when its coordinates and axis length satisfy the relationship $\delta_\alpha \sqrt{(c-1)/(p_\beta N^2)} = \delta_\beta \sqrt{(c-1)/(p_\alpha N^4)}$, the area of the rectangle surrounded by the points is the largest. Therefore, when the channel correlation is c , the sampling interval of the achievable maximum quantization area on the α - β domain can be calculated as

$$\Delta\alpha = \frac{1}{N^2} \sqrt{\frac{2(c-1)}{p_\alpha}}, \quad \Delta\beta = \frac{1}{N} \sqrt{\frac{2(c-1)}{p_\beta}}. \quad (38)$$

Consider that the user distribution is within a range of $r \in [\sqrt{0.62D^3/\lambda}, \infty)$ distance and angle of $\theta \in [-\pi/2, \pi/2]$. The maximum quantization range on α and β domain can be respectively calculated as

$$Q_\alpha = \sqrt{\frac{\lambda}{2.48D^3}} \approx \frac{1}{N\sqrt{N}}, \quad Q_\beta = 2. \quad (39)$$

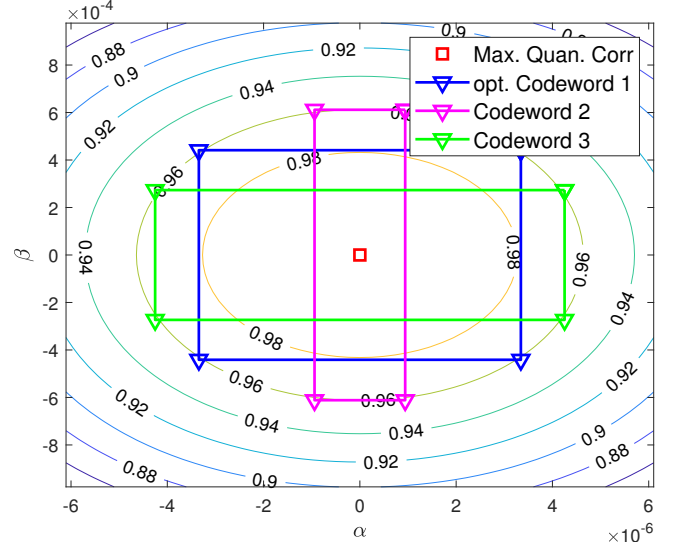


Fig. 7: Different codebook schemes under minimum quantization correlation c .

Then, the number of codewords in the α domain and β domain are given by

$$S_\alpha = \frac{Q_\alpha}{\Delta\alpha} = \sqrt{\frac{Np_\alpha}{2(c-1)}}, \quad S_\beta = \frac{Q_\beta}{\Delta\beta} = N\sqrt{\frac{2p_\beta}{(c-1)}}. \quad (40)$$

Thus, the total number of codewords to achieve the minimum number of feedback bits can be calculated as

$$S_{ULA} = S_\alpha S_\beta = \frac{N\sqrt{Np_\alpha p_\beta}}{(1-c)}. \quad (41)$$

At this time, the maximum quantization area of each codeword is

$$R_{max} = \frac{2(1-c)}{N^3} \sqrt{\frac{1}{p_\alpha p_\beta}}. \quad (42)$$

Therefore, for all sampling points of the ULA codebook, the coordinates of the s_α -th codeword in the α domain can be reformulated as

$$\alpha(s_\alpha) = \left(s_\alpha - \frac{1}{2}\right) \Delta\alpha, \quad s_\alpha = 1 \dots S_\alpha. \quad (43)$$

And the s_β -th codeword in the β domain can be reformulated as

$$\beta(s_\beta) = -1 + \left(s_\beta - \frac{1}{2}\right) \Delta\beta, \quad s_\beta = 1 \dots S_\beta. \quad (44)$$

(41) shows that the number of quantized bits of the codeword is only related to the channel correlation c and the number N of antennas but has nothing to do with the frequency. When the channel correlation c is constant, the number of codewords in the α domain is proportional to \sqrt{N} , and the number of codewords in the β domain is proportional to N . Moreover, if the number of antennas N remains unchanged, the channel correlation c increase can lead to an increase in the number of codebook quantization vectors.

It should be noted that, in the design of this scheme, for a fixed codeword quantization correlation, the number of

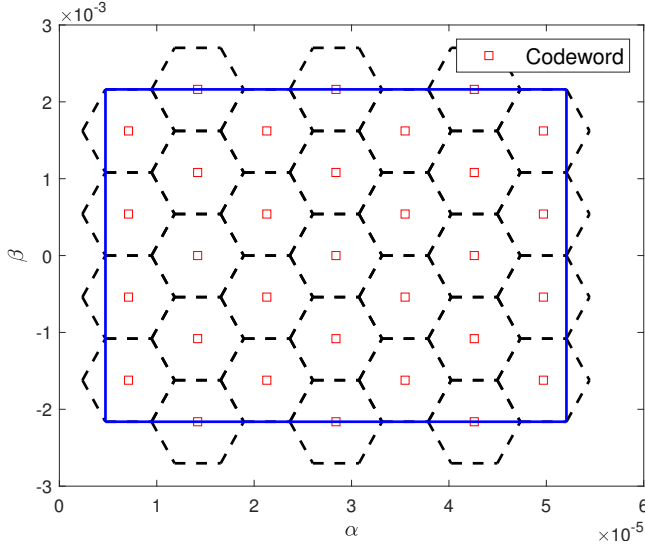


Fig. 8: Dislocation codewords on the α - β domain.

codewords in the β domain is always far greater than the number of codewords in the α domain. Therefore, under the same feedback bits, dense sampling in the β domain will be more conducive to improving the quantization performance of the codeword. In addition, if the minimum correlation is the same, quantizing $r \in [8, \infty)$ can save 1 bit of feedback than $r \in [4, \infty)$.

Example 1: In the case of the same channel correlation and different antenna array sizes, the optimal codeword numbers for the α domain and β domain are summarized in Table I, respectively. As the table shows, as the number of antennas and codewords on the α domain increase sequentially, the number of codewords on the β domain does not change much.

Table I: The number of codewords of the α domain and the β domain when the minimum correlation of codeword is 0.95.

	64	128	256	512
α domain	4	7	8	11
β domain	254	507	1014	2027

B. Dislocation Quantization Codebook Design Scheme

In the uniform quantization codebook design, the quantization region of each codeword is distributed in a rectangular shape. To further improve the accuracy of codeword quantized CSI, we propose a codebook design with dislocation. The quantization area of each codeword is distributed in a hexagon, which is symmetric about the a and b domains. $\Delta\alpha$ and $\Delta\beta$ are the sampling intervals of the offset codebook sampling scheme in the α and β domains, respectively. It should be noted that the dislocation here means that the codewords of the even or odd rows on the β domain are collectively shifted to the right by $\Delta\alpha/2$ along the α domain, as shown in Fig. 8.

Based on the hexagon's symmetry, the quantization area of a single codeword is always twice that of the inscribed triangle in Fig. 9. Therefore, the problem of maximizing the

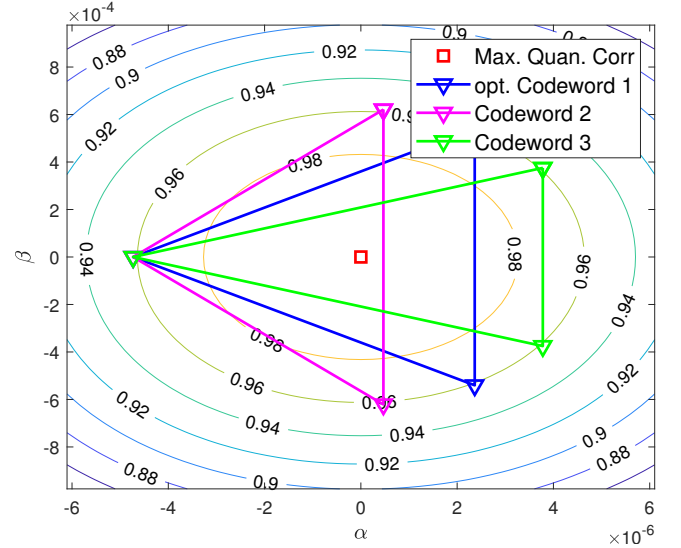


Fig. 9: Different codebook schemes with minimum quantization correlation c .

quantization area of a dislocation codeword can be transformed into the problem of finding the giant inscribed triangle of an ellipse. As mentioned above, based on Cauchy inequality, the codeword sampling steps in the α domain and β domain can be calculated as

$$\overline{\Delta\alpha} = \frac{3}{N^2} \sqrt{\frac{(c-1)}{p_\alpha}}, \quad \overline{\Delta\beta} = \frac{1}{N} \sqrt{\frac{3(c-1)}{p_\beta}}. \quad (45)$$

Under the maximum quantization area, the corresponding vertex of the quantization area of the codeword \mathbf{W}_0 is

$$\begin{aligned} (\alpha_1, \beta_1) &= \left(-\sqrt{\frac{c-1}{p_\alpha N^4}}, 0 \right), \\ (\alpha_2, \beta_2) &= \left(\frac{1}{2} \sqrt{\frac{c-1}{p_\alpha N^4}}, \frac{1}{2} \sqrt{\frac{3(c-1)}{p_\beta N^2}} \right), \\ (\alpha_3, \beta_3) &= \left(\frac{1}{2} \sqrt{\frac{c-1}{p_\alpha N^4}}, -\frac{1}{2} \sqrt{\frac{3(c-1)}{p_\beta N^2}} \right). \end{aligned} \quad (46)$$

Currently, the codeword is located at the center of gravity of the triangular quantization area. If codeword \mathbf{W}_0 is selected and used as the origin, then the position of the point with the minor channel correlation from the codeword under the two schemes satisfies the relationship as

$$f\left(-\frac{2}{3}\overline{\Delta\alpha}, 0\right) = f\left(\frac{1}{6}\overline{\Delta\alpha}, \frac{1}{2}\overline{\Delta\beta}\right). \quad (47)$$

Therefore, the maximum quantization area of a single codeword is

$$\overline{R}_{max} = \frac{3(1-c)}{2N^3} \sqrt{\frac{3}{p_\alpha p_\beta}}. \quad (48)$$

The number of the sampling points in the α and β domain is

$$\overline{S}_\alpha = \frac{1}{3} \sqrt{\frac{N p_\alpha}{(c-1)}}, \quad \overline{S}_\beta = 2N \sqrt{\frac{p_\beta}{3(c-1)}}. \quad (49)$$

And the number of codewords can be calculated as

$$\bar{S}_{ULA} = 2\bar{S}_\alpha\bar{S}_\beta = \frac{4N}{3(1-c)}\sqrt{\frac{Np_\alpha p_\beta}{3}}. \quad (50)$$

In the collection of ULA codewords, the coordinates of the s -th codeword in the α domain can be reformulated as

$$\alpha(\bar{s}_\alpha) = \begin{cases} (\bar{s}_\alpha - 1)\bar{\Delta}\alpha, & \text{odd row} \\ \frac{\bar{\Delta}\alpha}{6} + (\bar{s}_\alpha - 1)\bar{\Delta}\alpha, & \text{even row} \end{cases} \quad (51)$$

where $\bar{s}_\alpha = 1 \dots \bar{S}_\alpha$ and the t -th sampling point of the β domain can be reformulated as

$$\beta(\bar{s}_\beta) = \begin{cases} -1 + (\bar{s}_\beta - 1)\bar{\Delta}\beta, & \text{odd column} \\ -1 + \frac{\bar{\Delta}\beta}{2} + (\bar{s}_\beta - 1)\bar{\Delta}\beta, & \text{even column} \end{cases} \quad (52)$$

where $\bar{s}_\beta = 1 \dots \bar{S}_\beta$.

(41) and (50) provide the number of codewords under uniform and dislocation sampling. The number of dislocation sampling codewords is only 75% of the number of uniform sampling codewords. Therefore, in the same space, the dislocation quantization scheme can achieve the goal of low codebook quantization overhead by expanding the sampling interval of codewords.

V. NEAR-FIELD UPA CODEBOOK DESIGN

The non-stationary characteristic of the UPA channel correlation results in a different distribution for each codeword in 3D space. This section proposes the concept of a reference ellipsoid and assumes that the correlation formula for each codeword is always the same as the reference ellipsoid. Based on this assumption of stationarity, uniformly sampled codewords can be obtained. In this scheme, each codeword in the non-stationary UPA channel can meet the minimum correlation requirement.

A. Definition of Reference Ellipsoid

Proposition 1 shows that for any codeword, the pointing position of the channel vector that satisfies the minimum quantization correlation of c is always uniformly distributed on an ellipsoid centered around the quantization center of the codeword. It should be noted that due to the non-stationary characteristics of UPA channels, the size of the ellipsoid enclosed by different codewords at the positions that meet the conditions under the same minimum quantization correlation is always different. Therefore, when designing the optimal sampling interval between UPA codewords, the correlation feature of any codeword cannot be directly regarded as the correlation feature of all codewords, just like in ULA codebooks. In order to solve the problem caused by non-stationary features when designing the optimal sampling interval for codebooks, we hope to find a reference ellipsoid to describe the quantization features of any codeword in space. This reference ellipsoid provides the maximum allowable space, ensuring that all codewords can guarantee the minimum quantization correlation c at this volume. Below, we define a reference ellipsoid.

Definition 1: Consider sampling S_ψ , S_φ and S_ρ points on the ψ , φ and ρ domains, respectively. Using the channel

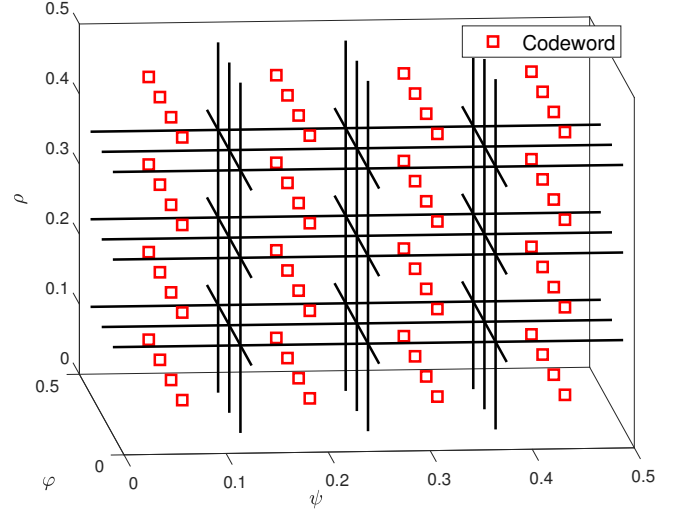


Fig. 10: Sampling points distribution in 3D space.

vector pointed at by the sampling point as the codeword, a total of $S^* = S_\psi S_\varphi S_\rho$ can be obtained. From Proposition 2, it can be concluded that when the quantization performance of all codewords satisfies the minimum correlation c^* , the sets of ellipsoidal axis lengths enclosed by the quantization boundaries of all codewords are respectively represented as $\mathbf{L}_\psi = \{l_{\psi,1}, \dots, l_{\psi,S_\psi}\}$, $\mathbf{L}_\varphi = \{l_{\varphi,1}, \dots, l_{\varphi,S_\varphi}\}$, $\mathbf{L}_\rho = \{l_{\rho,1}, \dots, l_{\rho,S_\rho}\}$. Meanwhile, $l_\psi^* = \min \mathbf{L}_\psi$, $l_\varphi^* = \min \mathbf{L}_\varphi$ and $l_\rho^* = \min \mathbf{L}_\rho$ are used as the axial length of the reference ellipsoid, then the formula of the reference ellipsoid can be written as

$$\frac{\delta_{\psi_s}^2}{(l_\psi^*)^2} + \frac{\delta_{\varphi_s}^2}{(l_\varphi^*)^2} + \frac{\delta_{\rho_s}^2}{(l_\rho^*)^2} = 1. \quad (53)$$

According to the fitting formula given in Proposition 2, the fitting coefficient can be calculated as

$$p_\psi^* = \frac{c-1}{(l_\psi^* N)^2}, \quad p_\varphi^* = \frac{c-1}{(l_\varphi^* N)^2}, \quad p_\rho^* = \frac{c-1}{(l_\rho^* N)^2}. \quad (54)$$

The formula for the reference ellipsoid can be completed as

$$\frac{\delta_{\psi_s}^2}{\frac{c-1}{p_\psi^* N^2}} + \frac{\delta_{\varphi_s}^2}{\frac{c-1}{p_\varphi^* N^2}} + \frac{\delta_{\rho_s}^2}{\frac{c-1}{p_\rho^* N^4}} = 1. \quad (55)$$

It is worth noting that some codewords may not achieve the expected minimum quantization correlation c when considering the ellipse whose axis length is longer than the axis length of the reference ellipse to represent the quantized region of the codeword. Therefore, the reference ellipsoid is the lower bound that can describe the quantization region of the codeword. The reference ellipsoid is a virtual ellipsoid reconstructed by taking the minimum value of the quantized region of all codewords, which may not exist.

B. Uniform Codebook Quantization Scheme

For the UPA channel model, UE is located at $r \in [\sqrt{0.62D^3/\lambda}, \infty)$ in distance, $[-\pi/2, \pi/2]$ in elevation angle and $[0, \pi]$ in azimuth angle. At this moment, the UE can be considered uniformly distributed in 3D space of $\psi \in [-1, 1]$,

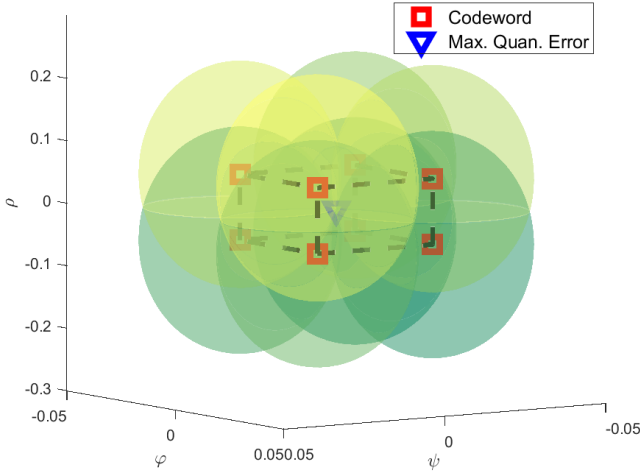


Fig. 11: Correlation distribution of eight adjacent uniform sampling points.

$\varphi \in [-1, 1]$ and $\rho \in [\sqrt{\lambda/0.62D^3}, \infty)$. Assuming that the codeword sampling step in the ψ domain, φ domain, and ρ domain is $\Delta\psi$, $\Delta\varphi$, and $\Delta\rho$. Respectively, the collection of sampling points can be represented as

$$\Xi^A = \left\{ (\psi_s, \varphi_s, \rho_s) \middle| \begin{aligned} \psi_s &= \psi_{min} + \frac{\Delta\psi}{2}, \psi_{min} + \frac{3\Delta\psi}{2}, \dots, \\ &\psi_{max}; \varphi_s = \varphi_{min} + \frac{\Delta\varphi}{2}, \varphi_{min} + \frac{3\Delta\varphi}{2}, \dots, \varphi_{max}; \\ \rho_s &= \rho_{min} + \frac{\Delta\rho}{2}, \rho_{min} + \frac{3\Delta\rho}{2}, \dots, \rho_{max} \end{aligned} \right\}. \quad (56)$$

Next, we provide a design for the UPA codebook. Considering a codebook design scheme for uniform sampling in the transform domain, as shown in Fig. 10. Among them, the red rectangle represents the codeword, and the solid black line represents the dividing line of the codeword quantization area. Assuming that the UPA channel is stationary, with a minimum correlation of c for all codewords, the quantization regions of all codewords are distributed in an ellipsoid of the same shape centered on the codeword, as shown in Fig. 11. For adjacent eight codewords, the boundaries of the quantization region of the codeword always intersect at one point under the same minimum quantization correlation c . Moreover, the intersection point is located at the center of a cuboid surrounded by eight adjacent codewords.

By distributing the features described in Fig. 11 throughout the entire space, it can be concluded that the quantization area of each codeword is enclosed in a cuboid. Moreover, the eight vertices of the quantized cuboid are located on the ellipsoidal boundary enclosed by the codeword under fixed correlation c .

When designing a codebook, higher quantization accuracy and less quantization overhead are always expected. With a fixed minimum quantization correlation, the larger the cuboid quantization area of the codeword in Fig. 11, the less quantization cost. For the enclosed cuboid of an ellipsoid, the maximum volume can be obtained when $\frac{c-1}{p_\rho^* N^4} \delta_{\varphi_s}^2 = \frac{c-1}{p_\psi^* N^2} \delta_{\rho_s}^2$

and $\frac{c-1}{p_\rho^* N^4} \delta_{\varphi_s}^2 = \frac{c-1}{p_\varphi^* N^2} \delta_{\rho_s}^2$ is satisfied. And the optimal sampling steps on the three domains can be calculated as

$$\begin{aligned} \Delta\psi &= \frac{2\sqrt{3}}{3N} \sqrt{\frac{c-1}{p_\psi^*}}, \\ \Delta\varphi &= \frac{2\sqrt{3}}{3N} \sqrt{\frac{c-1}{p_\varphi^*}}, \\ \Delta\rho &= \frac{2\sqrt{3}}{3N^2} \sqrt{\frac{c-1}{p_\rho^*}}. \end{aligned} \quad (57)$$

Therefore, the number of codewords in 3D space can be calculated as

$$S_\psi = \sqrt{\frac{3p_\psi^*}{c-1}} N, \quad S_\varphi = \sqrt{\frac{3p_\varphi^*}{c-1}} N, \quad S_\rho = 2.4 \sqrt{\frac{Np_\rho^*}{c-1}}. \quad (58)$$

The positions represented by the s_ψ -th, s_φ -th and s_ρ -th sampling points in ψ , φ and ρ domain can be expressed as

$$\begin{aligned} \psi(s_\psi) &= -1 + \left(s_\psi - \frac{1}{2}\right) \Delta\psi, s_\psi = 1, \dots, S_\psi, \\ \varphi(s_\varphi) &= -1 + \left(s_\varphi - \frac{1}{2}\right) \Delta\varphi, s_\varphi = 1, \dots, S_\varphi, \\ \rho(s_\rho) &= \left(s_\rho - \frac{1}{2}\right) \Delta\rho, s_\rho = 1, \dots, S_\rho. \end{aligned} \quad (59)$$

For the proposed codebook scheme, the sampling step is only related to the number of antennas and the minimum correlation. The larger the number of antennas, the smaller the sampling step. However, for the maximum quantization error, the sampling step will increase with its value, and the number of codeword sampling points in a specific space will decrease.

When the correlation of UPA channels is regarded as approximately stationary for sampling, the designed codeword accuracy is always lower than the accuracy using other points as reference positions. Because under the same sampling interval, the actual minimum correlation of each codeword is more significant than the minimum correlation of the reference position, its quantization accuracy is also more significant than the quantization area of the reference codeword. Thus, under this reference ellipsoid, when the quantization error is c , the quantization accuracy of the approximately stationary UPA sampling method is the lower bound among all uniform sampling methods. The quantization region of the codeword approximated by stationarity is always smaller than or equal to the actual maximum quantization region of the codeword under the minimum quantization correlation c . Therefore, a single codeword's achievable minimum quantization correlation is always greater than or equal to c .

Example 2: When the channel correlation is 0.95, the table below illustrates the number of sampling points for codewords in the 3D space (refer to Table II). Notably, the number of codewords in the ψ and φ domains consistently exceed the number in the ρ domain. Additionally, the number of sampling points in the angular domain is larger than the number of antennas. Incorporating oversampling in the angle domain during the design of the UPA codebook can effectively enhance the quantization accuracy of codewords.

Table II: The number of codewords in 3D space when the correlation of codeword is 0.95.

	8*8	12*12	16*16	32*32
ψ/φ domain	39*39	59*59	78*78	156*156
ρ domain	2	3	3	4

VI. SIMULATION RESULTS

In this section, we provide the simulation results to illustrate the performance of the proposed codebook schemes for ULA and UPA systems. The central frequency is $f = 3\text{GHz}$. Define the signal-to-noise ratios (SNR) of the system as

$$SNR = \frac{P\eta N}{r^2\sigma^2}. \quad (60)$$

P is the transmit power and σ^2 is the noise power. The achievable rate is given by

$$R = \log_2 \left(1 + \frac{P\eta N |\mathbf{W}^H \mathbf{b}(r, \theta)|^2}{r^2\sigma^2} \right). \quad (61)$$

The simulation results are the average results of 1000 randomly distributed UE. Firstly, we analyze the codebook of the ULA channel. The number of BS antennas is set as $N = 512$. The range of UE locates randomly in the space spanned $(r, \theta) \in [\sqrt{0.62D^3/\lambda}, \infty) \times [-\pi/2, \pi/2]$. Next, we evaluate the performance of the proposed UPA channel codebook. Considering the system model in Fig. 12, the BS is configured with UPA, whose number of antenna is 16×16 . The elevation angle and azimuth angle of the UE is $\theta \in [-\pi/2, \pi/2]$ and $\phi \in [0, \pi]$, respectively. The distance between the BS and the UE distributes in $r \in [\sqrt{0.62D^3/\lambda}, \infty)$.

Fig. 12 illustrates the cumulative probability function (CDF) of quantized correlation with various codebooks. In order to provide a comparative analysis, we conduct simulations using several codebooks. Firstly, we consider a codebook with identical sampled points in the α and β domains. Additionally, we evaluate a codebook optimized using the Lloyd algorithm. The proposed dislocation codebook and uniform codebook are both quantized with $B = 15$ bits. It is worth noting that, with an equal number of quantization vectors, the dislocation codebook consistently outperforms the uniform codebook. The proposed uniform codebook comprised 2617 sampling points in the α domain and 14 sampling points in the β domain.

On the other hand, the dislocation quantization codeword contains 1912 sampling points in the α domain and 18 sampling points in the β domain. The number of sampling points in the α domain is significantly higher than in the β domain. This phenomenon highlights the robustness of near-field beamforming in the β domain, and the denser sampling of the β domain enhances codeword quantization accuracy. It is observed that the performance of the codebook employing N sampled points in both domains is considerably inferior to the proposed codebooks, even when employing a more significant number of quantization vectors. Furthermore, the proposed schemes demonstrate significant superiority over the Lloyd algorithm optimization scheme, which validates the effectiveness of our proposed codeword design.

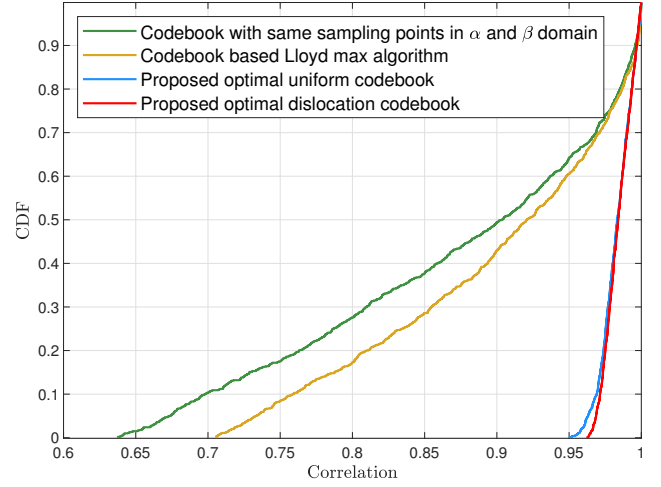


Fig. 12: CDF of the codebook quantization correlation in ULA channel.

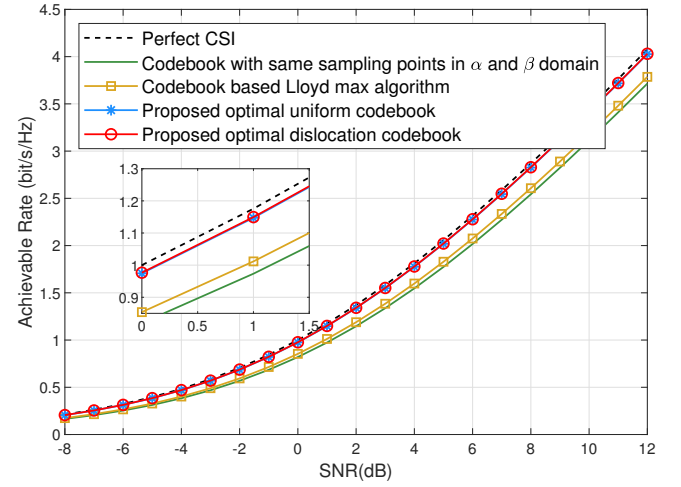


Fig. 13: Comparisons of average sum-rate against SNR for several codeword schemes in ULA channel, with $N = 512$ and $f = 3\text{GHz}$.

Fig. 13 illustrates the achievable rate for two scenarios: the ideal case of perfect channel state information (CSI) and the case where the precoding matrix is selected based on channel quantization. The beamforming scheme with perfect CSI represents the theoretical upper limit. In this comparison, we consider the same codebook scheme shown in Fig. 12. The proposed codebooks and the ideal case of perfect CSI exhibit remarkably similar performance. Notably, the dislocation codebook significantly enhances the achievable rate compared to the uniform codebook. When employing the same quantization bits, we observe that the achievable rate of the proposed uniform and dislocation codebook consistently outperforms the rate achieved using the Lloyd framework, particularly as the receiver SNR increases. Furthermore, the proposed codebook outperforms the codebook that employs the same sampling points in the α and β domains. The average sum rate demonstrates an improvement of approximately 0.4 bits/s/Hz compared to the codebook with the same sampling

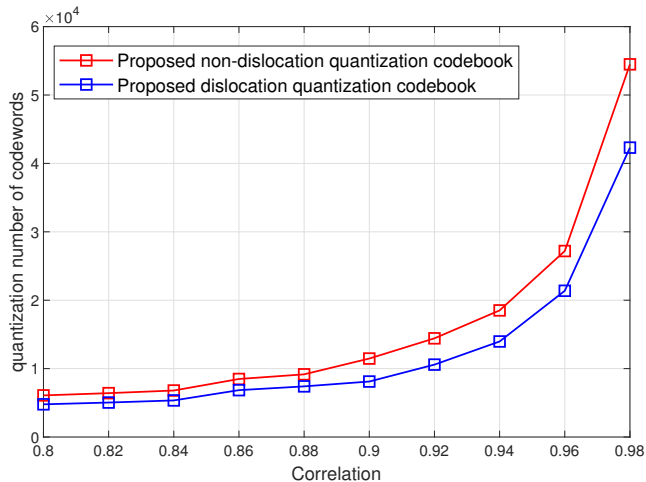


Fig. 14: Quantization Overhead consumption against the correlation of codebook.

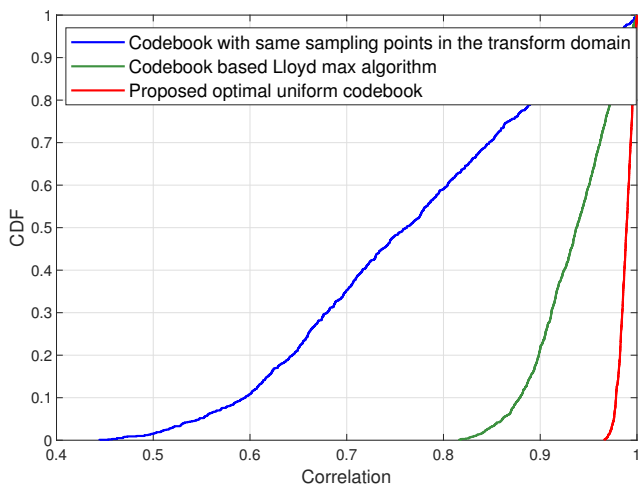


Fig. 15: CDF of the codeword quantification correlation in UPA channel, with $N_{BS} = 16 \times 16$, $f_c = 3GHz$.

points in the transformed domain.

In Fig. 14, we compare the number of quantization channel vectors of the proposed quantization schemes. The quantization vector's number of the proposed uniform codebook and dislocation codebook are respectively set according to (41) and (50). We observe that as the requirement for codebook quantization accuracy increases, the number of vectors required to quantize the channel also increases. The result shows that the dislocation codeword can approximately reduce the number of quantization bits by 25% compared with the uniform codeword, which is consistent with our analysis in Section IV.

We compare the proposed UPA codebook with two other schemes. In the first scheme, the codewords are uniformly sampled at N points in the ψ , φ , and ρ domains. The second scheme involves designing codewords with optimal sampling points based on the Lloyd algorithm in the ψ , φ , and ρ domains. Fig. 15 depicts the CDF of quantized correlation for the different codebooks. The quantized correlation achieved

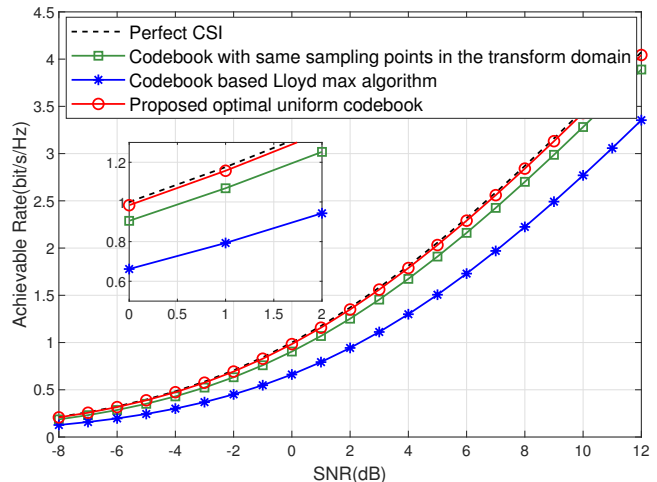


Fig. 16: Comparisons of average sum rate against SNR for several codebooks in UPA channel, with $N_{BS} = 16 \times 16$, $f_c = 3GHz$.

by the proposed uniform codebook is significantly superior to the other schemes. Following the codeword design scheme described in Section V, we assume a minimum codeword quantization correlation of $c = 0.95$. The simulation results consistently demonstrate that the quantized correlation achieved by the proposed codebook consistently exceeds 0.95. The result confirms that the proposed codebook is designed based on the lower bound of quantization correlation for all sampled codewords. Moreover, the proposed codebook exhibits more sampling points in the angle domain than in the distance domain. The results also reveal that the achievable rate performance of our proposed codebook consistently outperforms schemes with an equal number of samples in the ψ , φ , and ρ domains. Therefore, the near-field codebook should be oversampled in the angle domain. Considering the same quantization overhead, our proposed scheme achieves superior quantization correlation compared to the optimal codebook designed using the Lloyd Max algorithm.

We evaluate the average sum rate achieved by different codebooks when utilized as the beamforming matrix at the BS in the UPA system. Fig. 16 illustrates the results at various SNR. The outcomes demonstrate that our proposed UPA codebook scheme significantly outperforms the other two schemes and closely approaches the performance achieved with perfect CSI. Compared to the uniform codeword scheme, which employs the same number of samples in both the angle and distance domains, our proposed scheme exhibits an improvement of nearly 0.5 bits/s/Hz. Furthermore, our proposed codebook outperforms the codebook designed based on the Lloyd algorithm by more than 0.1 bits/s/Hz.

VII. CONCLUSION

This paper introduces a novel codebook design to maximize the minimum quantization correlation for quantized ELAA channels. We analyze the correlation between codewords and channel vectors and derive a suitable formula for this correlation. Based on these insights, we propose two

ULA codebooks: uniform sampling and dislocation sampling. Notably, the uniform offset codebook achieves the same quantization performance as the uniform codebook while requiring fewer quantization bits. Furthermore, our study reveals that the channel observed by the UPA exhibits non-stationarity. To address this, we propose a lower-bound scheme for optimally sampled codebooks. Additionally, we emphasize the robustness of the angle domain in ELAA systems and the advantages of oversampling the angle domain for codebook design with higher precision. Simulation results confirm that the proposed codebook achieves minimal quantization bits while maintaining the desired minimum quantization correlation.

REFERENCES

- [1] R. Chataut and R. Akl, "Massive MIMO systems for 5G and beyond networks—overview, recent trends, challenges, and future research direction," *Sensors*, vol. 20, no. 1, pp. 2753, May. 2020.
- [2] T. E. Bogale and L. B. Le, "Massive MIMO and mmWave for 5G wireless HetNet: Potential benefits and challenges," *IEEE Veh. Technol. Mag.*, vol. 11, no. 1, pp. 64–75, Mar. 2016.
- [3] C. E. De, A. Ali, A. Amiri, M. Angelichinoski, and R. W. Heath, "Non-stationarities in extra-large-scale massive MIMO," *IEEE Wirel. Commun.*, vol. 27, no. 4, pp. 74–80, Aug. 2020.
- [4] T. S. Rappaport, Y. Xing, O. Kanhere, S. Ju, A. Madanayake, S. Mandal, A. Alkhateeb and G. C. Trichopoulos, "Wireless communications and applications above 100 GHz: Opportunities and challenges for 6G and beyond," *IEEE access*, vol. 7, pp. 78729–78757, Jun. 2019.
- [5] M. Cui, Z. Wu, Y. Lu, X. Wei, and L. Dai, "Near-Field MIMO Communications for 6G: Fundamentals, Challenges, Potentials, and Future Directions," *IEEE Commun. Mag.*, vol. 61, no. 1, pp. 40–46, Sep. 2022.
- [6] K. T. Selvan and R. Janaswamy, "Fraunhofer and Fresnel Distances: Unified derivation for aperture antennas," *IEEE Antennas Propag. Mag.*, vol. 59, no. 4, pp. 12–15, Jun. 2017.
- [7] Y. Zhang, X. Wu and C. You, "Fast near-field beam training for extremely large-scale array," *IEEE Wireless Commun. Lett.*, vol. 11, no. 12, pp. 2625–2629, Oct. 2022.
- [8] C. A. Balanis, *Antenna theory: analysis and design*. John Wiley & sons, 2015.
- [9] N. Jindal, "Antenna combining for the MIMO downlink channel," *IEEE Trans. Wireless Commun.*, vol. 7, no. 10, pp. 3834–3844, Oct. 2008.
- [10] H. Zhang, N. Shlezinger, F. Guidi, D. Dardari, and Y. Eldar, "6G Wireless Communications: From Far-Field Beam Steering to Near-Field Beam Focusing," *6G Wireless Communications: From Far-Field Beam Steering to Near-Field Beam Focusing*, vol. 61, no. 4, pp. 72–77, Apr. 2023.
- [11] C. K. Wen, and W. T. Shih and S. Jin, "Deep learning for massive MIMO CSI feedback," *IEEE Wireless Commun. Lett.*, vol. 7, no. 5, pp. 748–751, Mar. 2018.
- [12] S. Schwarz, M. Rupp, S. Wesemann, "Grassmannian product codebooks for limited feedback massive MIMO with two-tier precoding," *IEEE J. Sel. Topics Signal Process.*, vol. 11, no. 5, pp. 1119–1135, Aug. 2019.
- [13] B. Ierckx and C. Oestges, *MIMO wireless networks: channels, techniques and standards for multi-antenna, multi-user and multi-cell systems*. Academic Press, 2013.
- [14] J. Kang and W. Choi, "Novel codebook design for channel state information quantization in MIMO rician fading channels with limited feedback," *IEEE Trans. Signal Process.*, vol. 69, pp. 2858–2872, May. 2021.
- [15] Y. Xie, S. Jin, J. Wang, Y. Zhu, X. Gao, and Y. Huang, "A limited feedback scheme for 3D multiuser MIMO based on Kronecker product codebook," in *Proc. IEEE Annu. Int. Symp. Pers. Indoor Mobile Radio Commun. (PIMRC)*, London, U.K., Sep. 2013, pp. 1130–1135.
- [16] R. M. Dreifuerst and R. W. Heath, "Initial Access Codebook Design and CSI Type-II Feedback for Sub-6GHz 5G NR," *arXiv preprint arXiv:2303.02850*, 2023.
- [17] *IEEE Standard for Local and metropolitan area networks Part 16: Air Interface for Broadband Wireless Access Systems Amendment 3: Advanced Air Interface*, IEEE Standard 802.16m, 2011.
- [18] Z. Xiao, T. He, P. Xia and X. G. Xia, "Hierarchical codebook design for beamforming training in millimeter-wave communication," *IEEE Trans. Wireless Commun.*, vol. 15, no. 5, pp. 3380–3392, Jan. 2016.
- [19] W. Shen, L. Dai, B. Shim, Z. Wang, and R. W. Heath, "Channel feedback based on AoD-adaptive subspace codebook in FDD massive MIMO systems," *IEEE Trans. Commun.*, vol. 66, no. 11, pp. 5235–5248, Jun. 2018.
- [20] P. H. Kuo, H. T. Kung and P. A. Ting, "Compressive sensing based channel feedback protocols for spatially-correlated massive antenna arrays," in *Proc. IEEE Wireless Commun. Netw. Conf. (WCNC)*, Shanghai, China, Apr. 2012, pp. 492–497.
- [21] X. Wei, L. Dai, Y. Zhao, G. Yu and X. Duan, "Codebook design and beam training for extremely large-scale RIS: Far-field or near-field?," *China Commun.*, vol. 19, no. 6, pp. 193–204, Jun. 2022.
- [22] S. Hu, M. C. Ilter, and H. Wang, "Near-Field Beamforming for Large Intelligent Surfaces," in *Proc. IEEE Annu. Int. Symp. Pers. Indoor Mobile Radio Commun. (PIMRC)*, Kyoto, Japan, Sep. 2022, pp. 1367–1373.
- [23] M. Cui and L. Dai, "Channel estimation for extremely large-scale MIMO: Far-field or near-field?," *IEEE Trans. Commun.*, vol. 70, no. 4, pp. 2663–2677, Jan. 2022.
- [24] X. Shi, J. Wang, Z. Sun and J. Song, "Hierarchical Codebook-based Beam Training for Extremely Large-Scale Massive MIMO," *arXiv preprint arXiv:2210.03345*, 2022.
- [25] W. U. Bajwa, J. Haupt, A. Sayeed, and R. Nowak, "Compressed Channel Sensing: A New Approach to Estimating Sparse Multipath Channels," *Proc. IEEE*, vol. 98, no. 6, pp. 1058–1076, Apr. 2010.
- [26] D. J. Love, R. Heath, and T. Strohmer, "Grassmannian beamforming for multiple-input multiple-output wireless systems," *IEEE Trans. Inf. Theory*, vol. 49, no. 10, pp. 2735–2747, Oct. 2003.
- [27] C. K. Au-yeung and D. J. Love, "On the performance of random vector quantization limited feedback beamforming in a MISO system," *IEEE Trans. Wireless Commun.*, vol. 6, no. 2, pp. 458–462, Feb. 2007.
- [28] P. Xia and G. Giannakis, "Design and analysis of transmit-beamforming based on limited-rate feedback," *IEEE Trans. Signal Process.*, vol. 54, no. 5, pp. 1853–1863, Apr. 2006.
- [29] Z. Wu and L. Dai, "Multiple Access for Near-Field Communications: SDMA or LDMA?," *IEEE J. Sel. Areas Commun.*, pp. 1 – 1, May. 2023.